Engineering Analysis with Boundary Elements 95 (2018) 40–52

Contents lists available at ScienceDirect

Engineering Analysis with Boundary Elements

journal homepage: www.elsevier.com/locate/enganabound

Global error analysis of two-dimensional panel methods for Neumann formulation

José M. Ezquerro, Victoria Lapuerta*, Ana Laverón-Simavilla, José J. Fernández

Universidad Politécnica de Madrid, Plaza de Cardenal Cisneros,3, Madrid 28040, Spain

ARTICLE INFO

Keywords:
Aerodynamics
Panel method
Asymptotic error
Global error
Potential flow

ABSTRACT

There are two main formulations for panel methods based on Green's formula: Dirichlet and Neumann methods. In a previous work a rigorous analytical study of the global error of Dirichlet method was performed. In this work an analytical study of the global error is performed for the other formulation: Neumann method. The analysis is performed for a wide variety of body shapes and different panel geometries to fully understand their effect on the convergence of the method. In particular, we study the global error associated with panel methods applied to thin or thick bodies with purely convex parts or with both convex and concave parts, and with smooth or non-smooth boundaries. In order to validate the analytical results, both numerical and analytical solutions for different body geometries have been considered to compare the actual and predicted errors in each case. Finally, a comparison of the error order between both methods, Dirichlet and Neumann, has also been performed for different configurations.

1. Introduction

Computational Fluid Models (CFDs) are widespread used in engineering practices, and especially in the field of aeronautics. However, they require long calculation times and the results are not always reliable, so inputs from other methods are often needed, as the methods for solving potential fluid flows.

The potential methods are valid only if the viscous effects are negligible or if they are reduced to small areas of the fluid field. In case of incompressible flows the velocity potential must satisfy the Laplace's equation. In case of linearised compressible subsonic flows, the velocity potential must satisfy the Prandtl–Glauert equation. In this last case, and by applying an easy transformation, the Prandtl–Glauert equation can be converted in the Laplace's equation, so that solving this last equation is enough to solve both kind of movements. The potential methods allow one to calculate numerically the solution of any given problem as long as the velocity potential satisfies the Laplace's equation.

The importance of the Laplace's equation in the aerodynamics (and many other scientific fields) had made the researchers to dedicate a great effort in developing analytical and numerical methods to solve this equation. One of the most developed potential methods is the panel method or boundary element method (BEM) [1,2], which reduce the problem of finding the velocity potential for the entire fluid to the calculation of this potential on the surface of the body itself. Thus, the dimension of the problem is reduced from three to two (or, in the case of two-dimensional flows, from two to one) making BEMs very attractive for their low computational cost compared with non-potential methods. Since the pioneering work of Hess and Smith there have been numerous publications and many numerical codes based on panel methods [3–14]; among these we emphasize the reviews of Hess [9], Erickson [10] and the book of Katz and Plotkin [12]. Boundary element methods are an active field of study, especially within the engineering community, with new applications being developed rapidly.

The panel method based on Green's formula was first introduced in the work of Morino and Kuo [4], in which the primary unknown was the velocity potential. There are two main formulations both based on Green's formula: Dirichlet and Neumann [12].The Dirichlet formulation solves the Laplace equation numerically and provides the velocity potential while with the Neumann formulation, only differences of potential are obtained. A lot of studies have addressed the question of error in these methods [15–21]. However, to the best of our knowledge, the first work that has tackled a rigorous analytical study of the global error of Dirichlet method is [22]. The analysis in that work was applied to thin or thick bodies, with purely convex parts or with both convex and concave parts, and with smooth or non-smooth boundaries.

A formal analytical estimation of the global error assumed when employing the Neumann formulation to solve the Green's integral equation is then the logical step forward. The solution of this system of equations

* Corresponding author.
E-mail addresses: jezquerro@eusoc.upm.es (J.M. Ezquerro), mariavictoria.lapuerta@upm.es (V. Lapuerta), ana.laveron@upm.es (A. Laverón-Simavilla), jose.ffraile@upm.es (J.J. Fernández).

https://doi.org/10.1016/j.enganabound.2018.06.019
Received 20 April 2018; Received in revised form 5 June 2018; Accepted 7 June 2018

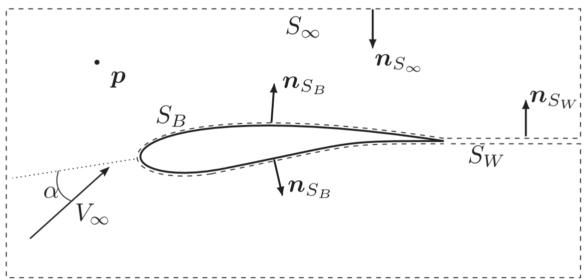

Fig. 1. Fluid domain in Green's integral equation. Sketch of the body and associated surfaces: body surface S_B, wake surface S_W and a surface at infinity S_∞. $\boldsymbol{V}_\infty$ and angle of attack, α, representation.

allows to obtain the differences of velocity potential values in a discretized domain derived from an obstacle embedded in a fluid domain.

This work presents a formal analytical and numerical analysis of the asymptotic global error in panel methods when applied to a Neumann formulation for different body geometries. The work is organized as follows. In Section 2 a brief description of panel methods is given. In Section 3 the global error analysis is performed analytically. In Section 4 the details of the error estimation are presented. Section 5 considers the numerical and analytical solutions for different body geometries in order to compare the actual and predicted errors in each case. In Section 6 a comparison between the error order of both formulations, Neumann and Dirichlet, is performed. Finally, in Section 7 the main conclusions are given.

2. Brief description of the panel method

In a previous work [22] the Green's integral equation:

$$\Phi(\boldsymbol{p}) = \int_{S_B} \frac{\partial \Phi}{\partial n} \Phi_m \, ds - \int_{S_B} \Phi \boldsymbol{\nabla} \Phi_m \cdot \boldsymbol{n} \, ds - (\Phi^+ - \Phi^-) \int_{S_W} \boldsymbol{\nabla} \Phi_m \cdot \boldsymbol{n} \, ds + \Phi_\infty, \tag{1}$$

was used to obtain the velocity potential Φ around a body of known shape submerged in a potential flow at any point $\boldsymbol{p}$ in space. This potential is considered to be caused by a distribution, on the surface of the body S_B, of point sources of intensity $\partial\Phi/\partial n$ and doublets of intensity Φ oriented along axes $\boldsymbol{n}$, and by a distribution, along the wake S_W, of doublets of intensity $\Phi^+ - \Phi^-$ with axis of orientation $\boldsymbol{n}$. Fig. 1 shows the body and the relevant surfaces; S_B is the body surface, S_W is a surface discontinuity of the velocity potential with two wet faces, also known as wake, and that connects S_∞ with S_B, S_∞ is the surface of the far field flow. The normal vector $\boldsymbol{n}$ on the body is oriented outward while it points upward along the wake, inward along the surface at infinity. Φ_m is the velocity potential produced at a point $\boldsymbol{p}$ by a point source of unit strength located on ds, $\boldsymbol{\nabla}\Phi_m \cdot \boldsymbol{n}$ is the velocity potential at a point $\boldsymbol{p}$ produced by a doublet of unit strength located on ds (at the body or at the discontinuity surface) and with its axis oriented along $-\boldsymbol{n}$, Φ^+ is the velocity potential on the upper side of the discontinuity surface S_W, and Φ^- on the lower one, and the final term in Eq. (1) is the potential of the stationary flow far from the body, evaluated at $\boldsymbol{p}$: $\Phi_\infty = U_\infty(x\cos\alpha + y\sin\alpha)$, where $U_\infty = |\boldsymbol{V}_\infty|$ and $\boldsymbol{V}_\infty$ is the fluid velocity at infinity, α is the angle between the incident flow and a reference line (angle of attack), and x and y are the coordinates of the point $\boldsymbol{p}$ in a fixed reference frame.

Imposing a vanishing normal velocity component on the boundary of the body,

$$\nabla\Phi \cdot \boldsymbol{n} = \partial\Phi/\partial n = 0, \tag{2}$$

and replacing this condition on Eq. (1), it becomes:

$$\Phi(\boldsymbol{p}) = -\int_{S_B} \Phi \boldsymbol{\nabla} \Phi_m \cdot \boldsymbol{n} \, ds - (\Phi^+ - \Phi^-) \int_{S_W} \boldsymbol{\nabla} \Phi_m \cdot \boldsymbol{n} \, ds + \Phi_\infty. \tag{3}$$

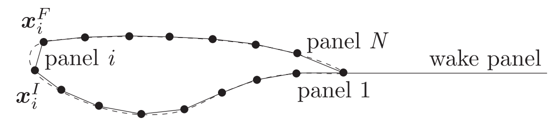

Fig. 2. Discretization of the body surface.

Eq. (3) represents the velocity potential Φ at a point $\boldsymbol{p}$ of a distribution of doublets on both the surface of the body and the discontinuity surface, with intensities Φ and $\Phi^+ - \Phi^-$ respectively and axis $\boldsymbol{n}$. Taking the point $\boldsymbol{p}$ to be on the surface of the body reduces the problem to an integral equation for the unknown velocity potential on the surface.

Eq. (3) can be written as

$$\Phi(\boldsymbol{p}) = \frac{1}{2\pi} \int_{S_B} \frac{\Phi(s)(\boldsymbol{p} - \boldsymbol{s}) \cdot \boldsymbol{n}}{|\boldsymbol{p} - \boldsymbol{s}|^2} ds + \frac{\Gamma}{2\pi} \int_{S_W} \frac{(\boldsymbol{p} - \boldsymbol{\xi}_w) \cdot \boldsymbol{n}_w}{|\boldsymbol{p} - \boldsymbol{\xi}_w|^2} d\xi_w + \Phi_\infty(\boldsymbol{p}), \tag{4}$$

where Φ_m and $\boldsymbol{\nabla}\Phi_m \cdot \boldsymbol{n}$ have been replaced by their mathematical expression. In the first integral, the variable of integration, s, is the arc length parameter along the body surface, $\boldsymbol{s} = \boldsymbol{s}(s)$ is a point on the body surface S_B, and $\boldsymbol{n} = \boldsymbol{n}(s)$ is the (unit) normal vector directed outward from that point. In the second integral the variable of integration is ξ_w, measuring distance along the wake panel S_W, while $\boldsymbol{\xi}_w = \xi_w(\xi_w)$ is a point on the wake panel and $\boldsymbol{n}_w$ is a unit normal vector directed upwards. The prefactor $\Gamma = \Phi^+ - \Phi^-$ denotes the circulation around the body.

Here we derive an estimate for the expected numerical error upon solving Eq. (4) with the lower order panel method. In what follows, the geometry of the body will be approximated with a collection of flat panels $\ell_i, i = 1..N$ of length l_i. We assume that the intensity of the doublet distribution is constant on each individual panel and that all panels are of comparable size, i.e, with a characteristic lengthscale $l = O(1/N)$; hereafter, we use the Landau notation "$O(\cdot)$" for order of magnitude. The discretization of the body surface and the wake are illustrated in Fig. 2.

Enumeration of the panels begins at the point of attachment of the wake, with panel number 1, and continues clockwise around the body, ultimately reaching the starting point again after panel N (this time from above the wake panel). As illustrated in Fig. 2, the endpoints of these panels (which lie on the body surface) similarly divide the true body surface into N (curved) segments L_i. We may thus decompose the first integral term in Eq. (4) to get

$$\Phi(\boldsymbol{p}) = \frac{1}{2\pi} \sum_{i=1}^{N} \int_{L_i} \frac{\Phi(s_i)(\boldsymbol{p} - \boldsymbol{s}_i) \cdot \boldsymbol{n}}{|\boldsymbol{p} - \boldsymbol{s}_i|^2} ds_i + \frac{\Gamma}{2\pi} \int_{S_W} \frac{(\boldsymbol{p} - \boldsymbol{\xi}_w) \cdot \boldsymbol{n}_w}{|\boldsymbol{p} - \boldsymbol{\xi}_w|^2} d\xi_w + \Phi_\infty(\boldsymbol{p}), \tag{5}$$

where we use the subscript i to indicate that $\boldsymbol{s}_i$ or s_i is restricted to the curved segment L_i.

The "numerical" potential $\Phi^n(\boldsymbol{p})$, is calculated by assuming a constant doublet distribution along each of the N panels ℓ_i. This latter potential can be written as

$$\Phi^n(\boldsymbol{p}) = \frac{1}{2\pi} \sum_{i=1}^{N} \Phi_i^n \int_{\ell_i} \frac{(\boldsymbol{p} - \boldsymbol{\xi}_i) \cdot \boldsymbol{n}_i}{|\boldsymbol{p} - \boldsymbol{\xi}_i|^2} d\xi_i + \frac{\Gamma^n}{2\pi} \int_{S_W} \frac{(\boldsymbol{p} - \boldsymbol{\xi}_w) \cdot \boldsymbol{n}_w}{|\boldsymbol{p} - \boldsymbol{\xi}_w|^2} d\xi_w + \Phi_\infty(\boldsymbol{p}), \tag{6}$$

where $\boldsymbol{\xi}_i$ is a point on panel i, with ξ_i measuring distance along it (see Appendix A.1 in [22] for more detail), $\boldsymbol{n}_i$ is an outward unit normal to this panel, and Γ^n is the numerically calculated circulation. The doublet strengths (potentials) Φ_i^n are determined by evaluating Eq. (6) at N collocation points, $\boldsymbol{x}_i$, one located on each of the N panels ℓ_i,

$$\Phi_i^n = \Phi^n(\boldsymbol{x}_i) = \frac{1}{2\pi} \sum_{j=1}^{N} \Phi_j^n \int_{\ell_j} \frac{(\boldsymbol{x}_i - \boldsymbol{\xi}_j) \cdot \boldsymbol{n}_j}{|\boldsymbol{x}_i - \boldsymbol{\xi}_j|^2} d\xi_j + \frac{\Gamma^n}{2\pi} \int_{S_W} \frac{(\boldsymbol{x}_i - \boldsymbol{\xi}_w) \cdot \boldsymbol{n}_w}{|\boldsymbol{x}_i - \boldsymbol{\xi}_w|^2} d\xi_w + \Phi_\infty(\boldsymbol{x}_i), \tag{7}$$